# A New Series of Cu(II) Coordination Polymers Derived from Bis-pyridyl-bis-urea Ligands and Various Dicarboxylates and Their Role in Methanolysis of Epoxide Ring-Opening Catalysis

Subhabrata Banerjee, Dhurjati Prasad Kumar, Sabyasachi Bandyopadhay,[#] N. N. Adarsh,[§] and Parthasarathi Dastidar*

Department of Organic Chemistry, Indian Association for the Cultivation of Science (IACS), 2A & 2B Raja S C Mullick Road, Jadavpur Kolkata −700032, West Bengal, India

Ⓢ *Supporting Information*

ABSTRACT: A crystal engineering approach has been adopted in synthesizing six new mixed ligand based Cu(II) coordination polymers (CPs) derived from two bis-pyridyl-bis-urea ligands, namely, *N,N′*-bis-(3-pyridyl)ethylene-bis-urea (**L1**) and *N,N′*-bis-(3-pyridyl)propylene-bis-urea (**L2**), and various dicarboxylates. The single crystal structures of the coordination polymers displayed diverse supramolecular architectures such as a one-dimensional (1D) chain, 1D-looped chain, and two-dimensional grid. Although none of them displayed an open-framework structure, which is believed to be conducive for heterogeneous catalysis, almost all of them showed moderate to excellent epoxide ring-opening catalysis. Powder X-ray diffraction indicated structural changes/degradation of the CPs, which might be generating substrate accessible Cu(II) species that presumably acted as the catalyst.
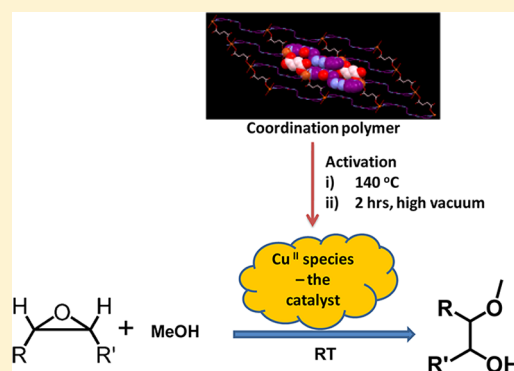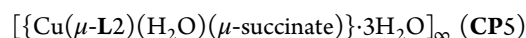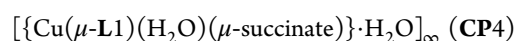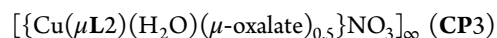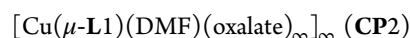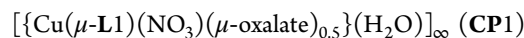
INTRODUCTION

Coordination polymers (CPs) are hybrid solids with infinite network structures built from organic bridging ligands (linker) and metal ions (node).[1] In recent years, CPs received a considerable attention owing to their various potential applications.[2a−d] The last decade has witnessed an upsurge of research activities involving the synthesis of intriguing CPs derived from ligands equipped with hydrogen bonding functionality (noninnocent backbone-NIB). The NIB backbone of the ligands is shown to participate in complementary hydrogen bonding interactions resulting in internetwork hydrogen bonding.[3] However, such occurrence of internetwork hydrogen bonding is not so common as the NIB of ligands might also particiapte in hydrogen bonding interactions with guests (solvents) molecules and/or counteranions. Such CPs displayed interesting structures and functions.[4] To promote internetwork hydrogen bonding, two strategies have been adopted: (i) by increasing the number of hydrogen bonding funtionality (e.g., from mono to bis-functionalized ligands), the internetwork interactions could be achieved[5] and (ii) by employing bis-anionic coligands such as dicarboxyates in mixed ligand systems, it was possible to avoid NIB−counteranion interactions.[6] Urea has a well studied hydrogen bonding functionality that usually displays a 1D hydrogen bonded network as shown in Scheme 1. To explore the role of urea in a mixed ligand systems, we decided to exploit two bis-pyridyl-bis-urea ligands, namely, *N,N′*-bis-(3-pyridyl)ethylene-bis-urea (**L1**) and *N,N′*-bis-(3-pyridyl)propylene-bis-urea (**L2**), in

Scheme 1
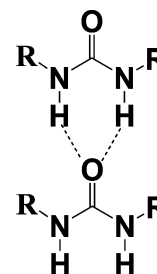
synthesizing neutral mixed ligand CPs wherein oxalate, succinate, and 2,6-naphthalene dicarboxylate were used as coligands (Scheme 2). Thus, a new series of Cu(II) CPs, namely,

$[\{Cu(\mu\text{-}\mathbf{L1})(NO_3)(\mu\text{-oxalate})_{0.5}\}(H_2O)]_{\infty}$ (**CP1**)

$[Cu(\mu\text{-}\mathbf{L1})(DMF)(oxalate)_{\infty}]_{\infty}$ (**CP2**)

$[\{Cu(\mu\mathbf{L2})(H_2O)(\mu\text{-oxalate})_{0.5}\}NO_3]_{\infty}$ (**CP3**)

$[\{Cu(\mu\text{-}\mathbf{L1})(H_2O)(\mu\text{-succinate})\}\cdot H_2O]_{\infty}$ (**CP4**)

$[\{Cu(\mu\text{-}\mathbf{L2})(H_2O)(\mu\text{-succinate})\}\cdot 3H_2O]_{\infty}$ (**CP5**)

[{Cu(μ-**L1**)(μ-2, 6-naphthalene dicarboxylate)H$_2$O}·2MeOH]$_\infty$ (**CP6**)
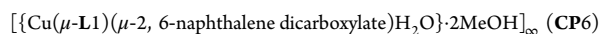
Scheme 2
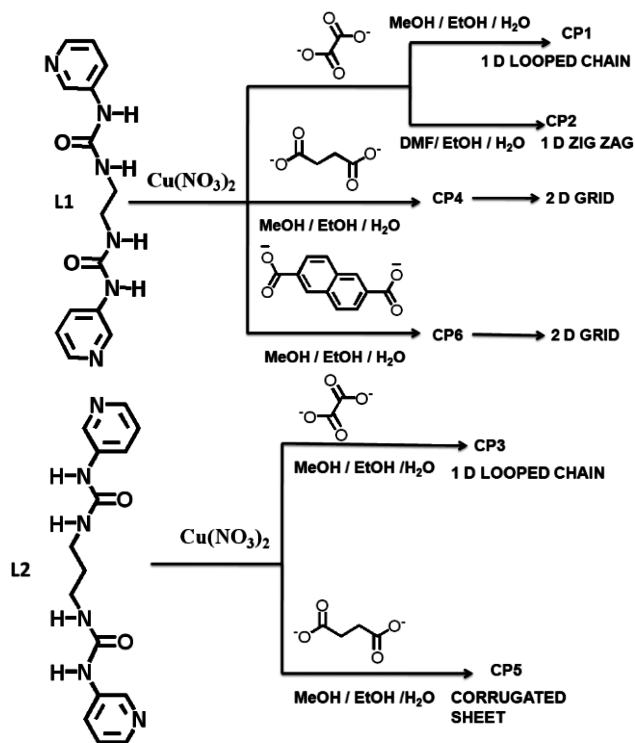
have been synthesized and structurally characterized mainly by single crystal X-ray diffraction (SXRD). It may be noted that while **L1** has been utilized to generate various CPs useful in anion chemistry,[7a−c] **L2** remains unexplored in the coordination polymer literature; only the structure of **L2** is reported.[7a] No mixed ligand based CPs have been reported involving these two ligands as per CSD search. Interestingly, these CPs displayed catalytic behavior in ring-opening methanolyses of epoxides.

■ RESULTS AND DISCUSSION

We reacted separately **L1** and **L2** with various dicarboxylates and Cu(NO$_3$)$_2$ in a 1:0.33:1 (ligand/carboxylate/metal) molar ratio. It was noted that CP synthesis trials with a 1:1:1 (ligand/carboxylate/metal) molar ratio lead to the formation of CPs having only carboxylate ligands in most of the cases. However, reducing the amount of the carboxylates as stated above, we could isolate the corresponding mixed ligand CPs **CP1**−**CP6**. Suitably grown single crystals of the CPs were then subjected to SXRD experiments (see Table 1).

Crystal Structure of [{Cu(μ-L1)(NO$_3$)(μ-oxalate)$_{0.5}$}-(H$_2$O)]$_\infty$ (CP1). Reaction of **L1** and dipotassium oxalate with Cu(NO$_3$)$_2$ in aqueous MeOH/EtOH mixture resulted in X-ray quality crystals (green, block shaped) of **CP1**. SXRD data revealed that the crystal belonged to the centrosymmetric triclinic space group $P\bar{1}$. The asymmetric unit contained one ligand, half oxalate molecule residing on a center of symmetry, one nitrate counteranion coordinated to the metal center, one solvate water molecule, and some smeared electron densities that could not be modeled. SQUEEZE[8] calculations revealed the presence of 16 e in the unit cell, which was attributed to 0.8 water molecule in the asymmetric unit. Subsequent thermog-

ravimetric (TG) data showed a weight loss of 12.4%, which did not match with the calculated value of 6.4% (considering one solvate water molecules and 0.8 water from SQUEEZE calculation). This could be due to the fast desolvation of loosely bound water molecules in the lattice. The ligand adopted an overall V-shaped geometry presumably because of the *gauche* conformation of its ethylene backbone. The relative orientation of the pyridyl N and urea O atoms may be best described as *syn-syn*. The pyridyl and urea plane in each terminal were found to be reasonably planar with the corresponding dihedral angles of 17.8 and 22.9°, whereas the dihedral angles involving terminal pyridyl rings and urea moieties were 79.2 and 85.9°, respectively. The metal center Cu^{II} showed a distorted square pyramidal geometry wherein the apical site was occupied by labile nitrate counteranion and the equatorial sites were occupied by pyridyl N and oxalate O atoms. The oxalate moiety was found be involved in extended coordination bond via chelate mode wherein the O atoms came from both the terminal carboxylates. The overall network may best described as 1D looped chain topology wherein each loop was completed by the pyridyl ligands and bridged by oxalate. The metal−metal distance in the loop was 14.12 Å. The looped chains were packed in parallel fashion sustained by various hydrogen bonding interactions involving urea N, oxalate O, and nitrate O and solvate water O atoms. While one of the urea N−H moieties was involved in hydrogen bonding with the carboxylate O [N···O = 2.919(5) Å, ∠N−H···O = 142.8(2)°] and lattice occluded water [N···O = 3.010(5) Å, ∠N−H···O = 167.5(1)°], the other one made short contact with the O atom of nitrate counteranion [N···O = 2.970(5) Å, ∠N−H···O = 133.7 (1)°]; one of the urea >C═O moieties interacted with the solvate water molecule via O−H···O interactions [O···O = 2.7996 Å], while the other one remained free from any hydrogen bonding interactions (Figure 1).

Crystal Structure of [Cu(μ-L1)(DMF)$_2$(oxalate)]$_\infty$ (CP2). Interestingly when we changed one of the crystallization solvents (DMF instead of MeOH) keeping the rest of the reaction conditions identical as in the case of **CP1**, crystals of **CP2** were formed. The space group of **CP2** was found to be the centrosymmetric triclinic $P\bar{1}$. The asymmetric unit contained one molecule of **L1**, one oxalate coordinated to the metal center in a chelate fashion, and two DMF molecules coordinated to the metal center. The final electron density map in SXRD data was clean indicating no solvent occlusion. TG data also supported the SXRD data; a weight loss of 12.6% attributed to the two coordinated DMF molecules exactly matched with the calculated value of 12.4%. The ligand displayed a V-shaped conformation presumably due to the *gauche* conformation of the ethylene backbone. It also adopted a *syn-anti* conformation with respect to the relative orientation of the pyridyl N and urea O atoms. The terminal pyridyl moieties were found to be relatively planar with corresponding urea moieties; the dihedral angles involving these moieties were 14.3 and 22.6°. The dihedral angle involving the terminal pyridyl rings and urea moieties were 68.78 and 64.45°. The metal center geometry may be best described as slightly distorted octahedral wherein the apical positions were coordinated by the O atoms of the DMF molecules and the equatorial positions were occupied by the N atoms of pyridyl rings and O atoms of oxalate. The overall extended coordination via pyridyl atoms resulted in the formation of a 1D wavy CP. The neighboring 1D chains further packed in a parallel fashion sustained by hydrogen bonding involving urea

Table 1. Crystallographic Parameter Table CP1−CP6

crystal parameters	CP1	CP2	CP3	CP4	CP5	CP6
CCDC No.	885295	885294	885297	885296	885298	885293
empirical formula	C15 H20 Cu N7 O9	C22 H30 Cu N8 O8	C16 H20 Cu N7 O8	C18 H20 Cu N6 O10	C19 H30 Cu N6 O10	C26 H26 Cu N6 O8
formula weight	505.92	598.08	501.93	543.94	566.03	614.07
crystal size/mm	0.29 × 0.22 × 0.14	0.20 × 0.10 × 0.06	0.28 × 0.21 × 0.12	0.32 × 0.26 × 0.17	0.40 × 0.26 × 0.12	0.26 × 0.14 × 0.10
crystal system	triclinic	triclinic	triclinic	triclinic	orthorhombic	triclinic
space group	$P\bar{1}$	$P\bar{1}$	$P\bar{1}$	$P\bar{1}$	$Pca2_1$	$P\bar{1}$
a (Å)	8.8618(13)	8.2254(4)	9.5396(8)	8.3131(8)	18.4348(9)	9.6440(8)
b (Å)	9.4700(14)	11.6133(6)	9.7085(8)	8.4982(8)	7.9490(4)	10.2113(8)
c (Å)	12.5265(18)	14.3603(8)	12.6295(12)	8.8252(8)	15.9297(8)	10.4677(9)
$\alpha/0$	102.496(4)	76.278(2)	74.927(2)	69.901(2)	90.00	102.075(2)
$\beta/0$	93.441(4)	86.541(2)	76.612(2)	86.713(2)	90.00	116.625(2)
$\gamma/0$	94.785(4)	76.787(2)	87.388(2)	82.023(2)	90.00	106.280(2)
volume (Å³)	1019.5(3)	1297.30(12)	1098.61(17)	579.80(9)	2334.3(2)	814.46(12)
Z	2	2	2	1	4	1
F(000)	520	622	516	279	1180	317
μ MoKα (mm^{-1})	1.137	0.905	1.051	0.844	1.004	0.721
temperature/K	298(2)	298(2)	298(2)	298(2)	298(2)	298(2)
R_{int}	0.0725	0.0281	0.0353	0.0296	0.0422	0.0543
range of h, k, l	−9/8, −10/10, −13/13	−9/9, −13/13, −17/17	−11/11, −11/11, −14/14	−9/9, −10/10, −10/10	−24/24, −10/10, −20/19	−10/10, −11/10, −11/11
$\theta_{\text{min/max}}$ (°)	1.67/23.00	1.46/25.00	1.71/24.97	2.46/24.99	2.21/28.05	2.26/22.88
reflections collected/unique/observed [$I > 2\sigma(I)$]	8163/2820/1910	12056/4561/3866	13046/3830/3169	5456/2023/1699	25087/5276/4708	8021/2234/1839
data/restraints/parameters	2820/0/280	4561/0/356	3830/0/297	2023/0/387	5276/0/403	1839/0/187
goodness of fit on F^2	1.006	1.070	1.029	1.042	0.992	0.969
final R indices [$I > 2\sigma(I)$]	$R_1 = 0.0491$ $wR_2 = 0.0882$	$R_1 = 0.0314$ $wR_2 = 0.0792$	$R_1 = 0.0333$ $wR_2 = 0.0776$	$R_1 = 0.0435$ $wR_2 = 0.1251$	$R_1 = 0.0283$ $wR_2 = 0.0635$	$R_1 = 0.0431$ $wR_2 = 0.1027$
R indices (all data)	$R_1 = 0.0823$ $wR_2 = 0.0987$	$R_1 = 0.0844$ $wR_2 = 0.0792$	$R_1 = 0.0823$ $wR_2 = 0.0987$	$R_1 = 0.0531$ $wR_2 = 0.1329$	$R_1 = 0.0343$ $wR_2 = 0.0662$	$R_1 = 0.0568$ $wR_2 = 0.1094$
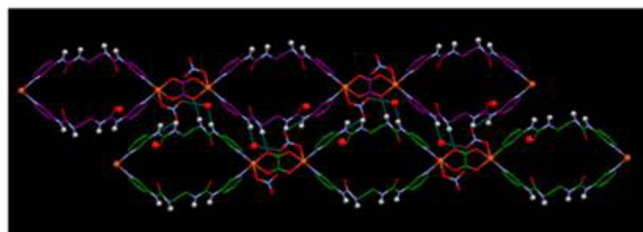
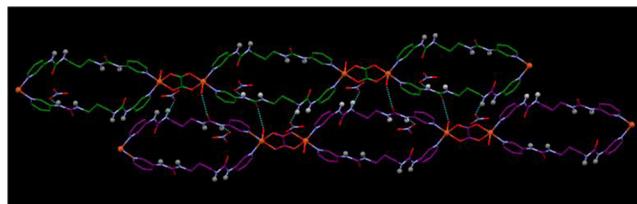**Figure 1.** Parallel packing of 1D looped chains in CP1 displaying various hydrogen bonding (⋯) interactions.

N and oxalate O atoms [N⋯O = 2.834–3.095 Å, ∠N–H⋯O = 136.9 (2)–146.1 (2)°] (Figure 2).
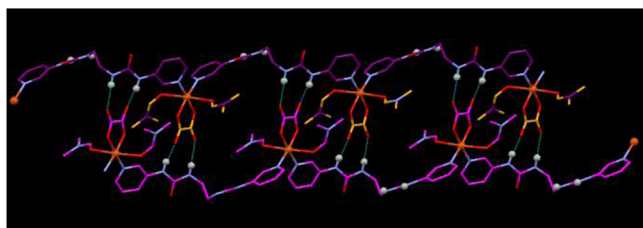
Figure 2. Parallel packing of the 1D chain in CP2 displaying hydrogen bonding (⋯) involving urea and oxalate.

Crystal Structure of [{Cu(μ-L2)(H₂O)(μ-oxalate)₀.₅}-NO₃]∞ (CP3). When **L2** was used instead of **L1** in an identical condition of synthesizing **CP1**, crystals of **CP3** were obtained. SXRD revealed that the crystals belonged to the centrosymmetric triclinic space group $P\bar{1}$. In the asymmetric unit, one ligand, half a molecule of oxalate (residing on a center of symmetry), one water molecule coordinated to the metal center and one free nitrate counteranion were located. The final electron density map was found be clean indicating absence of lattice included solvents. A weight loss of 3.5% attributed to one coordinated water molecule (calc. 3.6%) in TG data supported the crystal structure. The ligand adopts a V-shaped geometry presumably due to the *gauche* and *staggered* conformation of the propylene backbone. It also displayed *anti-syn* conformation with respect to the relative orientation of the pyridyl N and urea O atoms. In this case also, the terminal pyridyl rings and urea moieties were found to be planar displaying dihedral angles of 15.3 and 9.1°. The terminal pyridyl rings and urea moieties display dihedral angles of 62.8 and 61.3°, respectively. The metal center adopted a distorted square pyramidal geometry wherein the apical position was occupied by a water molecule and the equatorial sites were coordinated by pyridyl N and oxalate O atoms. Extended coordination by the pyridyl N and oxalate O atoms resulted in a 1D looped chain topology. The metal−metal distance was 16.87 Å, slightly longer than that of in **CP1**. The chains were packed in parallel fashion sustained by hydrogen bonding involving urea O atom and metal bound water [O⋯O 2.761(4)–3.064(4) Å, ∠O–H⋯O = 175.0(4)–177.0 (4)°], and the urea N atom and nitrate O atoms [N⋯O = 2.977(3)−3.170(3) Å, ∠N–H⋯O = 144.2 (2)−170.3 (2)°] (Figure 3).

Crystal Structure of [{Cu(μ-L1)(H₂O)₂(μ-succinate)}-H₂O]∞ (CP4). When the molecular length of the coligand increased as compared to oxalate such as in succinate, reaction of **L1** under identical conditions for the synthesis of **CP1** resulted in block-shaped blue crystals of **CP4**. SXRD indicated the centrosymmetric triclinic space group $P\bar{1}$. The asymmetric

Figure 3. Parallel packing of 1-D looped chains in CP3 displaying various hydrogen bonding (⋯) interactions.

unit contained half a molecule of **L1**, half coligand succinate (both residing on center of symmetry), one water molecule coordinated to a half occupied Cu^{II}, and a solvate water molecule. The final electron density map was clean. A weight loss of 10.5% in TG data clearly supported the loss of three water molecules (calc. 9.9%) as seen in the crystal structure. The ligand adopted an overall linear topology due to the staggered conformation of the ethylene backbone. The relative orientation of the pyridyl N and urea O atoms in each terminal was found to be syn−syn. However, anti orientation of the terminal pyridyl N atoms made the ligand have a linear ligating topology. Each pyridyl urea segment appears to be quite planar; the dihedral angles between the pyridyl ring and urea moiety were 5.9 and 6.6° and the terminal pyridyl rings and urea moieties made dihedral angles of 5.91°and 0.51°, respectively, among themselves. The metal center displayed a slightly octahedral geometry wherein the equatorial positions were occupied by pyridyl N and succinate O atoms and the apical positions were coordinated by water molecules. Because of extended coordination of the pyridyl ligand and succinate coligand, the crystal structure displayed a 2D grid architecture. However, there was no space available within the grid for guest occlusion. The 2D grids were packed in parallel fashion. The solvate water molecules were embedded within the interstitial space between the 2D layers sustained by extensive hydrogen bonding involving urea O [N⋯O = 2.991(4)Å, ∠N–H⋯O = 145.1 (1)°], succinate O [O⋯O = 2.7329 Å] and metal bound water molecule [O⋯O = 2.7329 Å] (Figure 4).

Crystal Structure of [{Cu(μ-L2)(H₂O)(μ-succinate)}·3-H₂O]∞ (CP5). When **L2** was reacted with Cu(NO₃)₂ under identical conditions of **CP4** synthesis, block shaped blue crystals of **CP5** were obtained. SXRD indicated that they
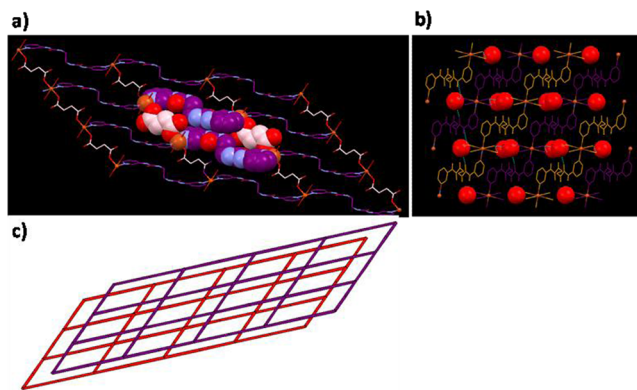
Figure 4. (a) 2D grid architecture displaying one grid in space-filling model, (b) parallel packing of the grids (shown in alternating orange and purple color) displaying the solvate water molecules (red ball) occupying the interstitial space sustained by various hydrogen bonding (⋯), (c) TOPOS[9] diagram of two offsetly packed 2D sheets in CP4.

belonged to the noncentric orthorhombic space group $Pca2_1$. The asymmetric unit contains one Cu^{II} metal center, one **L2**, one succinate, one metal bound water, and three solvate water molecules. The final refinement cycle did not show any significant electron density. TG data also supported the crystal structure [weight loss for four water molecules = 12.7% (expected), 12.8% (found)]. The propylene backbone displayed *gauche* and *staggered* conformation resulting in an overall V-shape in the molecule. The relative orientation of the pyridyl N and urea O atoms in each terminal was found to be *syn-syn*. However, *anti* orientation of the terminal pyridyl N atoms gave the molecule a linear ligating topology. Each pyridyl urea moiety displayed reasonably planar conformation; the dihedral angles between the pyridyl ring and urea moiety in each terminal were 17.5 and 14.3°. The dihedral angles between the urea moieties and pyridyl rings were 48.9 and 70.2°. The metal center displayed a slightly distorted square pyramidal geometry wherein the equatorial positions were occupied by succinate O and pyridyl N atoms and the apical position was coordinated by a water molecule. Because of the extended coordination involving both the pyridyl ligand and succinate coligand, the crystal structure displayed a grid architecture which had a highly undulating topology. In this case also, there was no space available within the grid. The solvate water molecules were located within the interstitial space available between the 2D grids which were parallelly packed. Extensive hydrogen bonding interactions involving urea N [N···O = 2.897(3)−3.081(3) Å, ∠N−H···O = 149.0 (4)−176.8(2)°] and O [O···O = 2.847(3)−2.790(3) Å, ∠O−H···O = 167(3)°] and succinate O [O···O = 2.695(2)−2.825(3) Å, ∠O−H···O = 164(3)−173(3)°] with the solvate water molecule were observed (Figure 5).
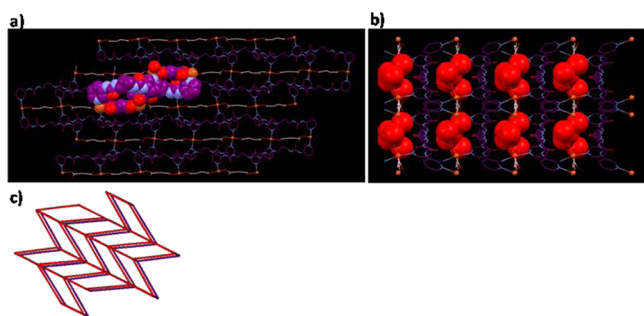
Figure 5. (a) 2D grid architecture displaying one grid in space-filling model, (b) parallel packing of the grids displaying lattice occluded water molecules (red balls) within the interstitial space, (c) TOPOS[9] view of the highly undulating grids.

Crystal Structure of [{Cu(μ-L1)(μ-naphthalene dicarboxylate)H₂O}·2MeOH]∞ (CP6). Reaction of **L1** with 2,6-naphthalene dicarboxylate under identical conditions for **CP1** synthesis resulted in block shaped bluish-green crystals of **CP6**. The space group was found to be the centrosymmetric triclinic $P\bar{1}$. The asymmetric unit contained half occupied Cu^{II}, half **L1**, half 2,6-naphthalene dicarboxylate, one metal bound water, and smeared electron densities that could not be modeled. The electrons (26 e/asymmetric unit) found in the SQUEEZE[8] calculations were assigned to two solvate MeOH. However, TG data were found to be inconsistent with the calculated results (calc. 12.6%; experimental 21.8%). This could be because of the difference in solvent loss in two different

experiments (SXRD and TG). The ligand adopted a *staggered* conformation in its ethylene backbone. The relative orientation of the pyridyl N and urea O atoms in each terminal was found to be *syn-syn*. However, the ligand molecule displayed a linear ligating topology because of the relative *anti* orientation of the pyridyl N atoms. Each pyridyl urea moiety displayed reasonably planar conformation; the dihedral angles between the pyridyl ring and urea moiety in each terminal were 0° and 0°. The dihedral angles between the urea moieties and pyridyl rings were 4.1 and 4.1°. The metal center displayed a distorted octahedral geometry wherein the equatorial positions were occupied by O atoms of 2,6-naphthalene dicarboxylate and water molecules and the apical positions were coordinated by pyridyl N atoms. Extended coordination involving both the pyridyl ligand and 2,6-naphthalene dicarboxylate resulted in 2D grid architecture. Interestingly, in this case there was a space of ~3.9 × 7.9 Å available for guest occlusion. The disordered electron densities were located within this space. The grids were packed in offset fashion sustained by hydrogen bonding involving urea N and 2,6-naphthalene dicarboxylate O [N···O = 2.947(4)−3.149(4) Å, ∠N−H···O = 151.1(1)−159.8 (1)°] atoms and C−H···π interactions involving naphthyl ring and pyridyl C−H (Figure 6).
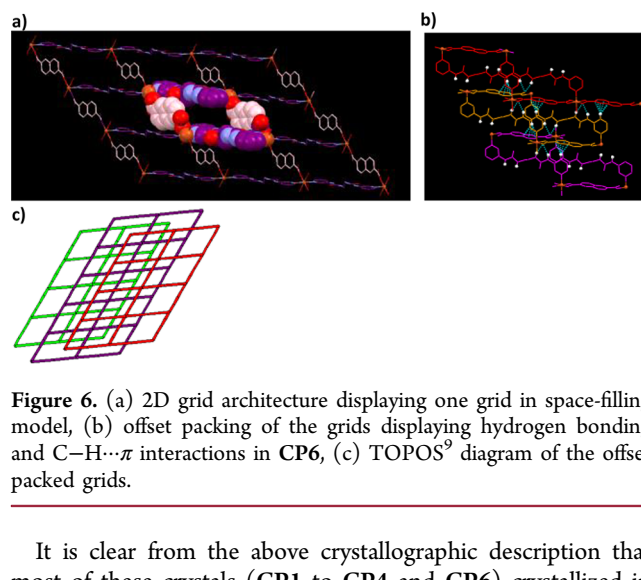

Figure 6. (a) 2D grid architecture displaying one grid in space-filling model, (b) offset packing of the grids displaying hydrogen bonding and C−H···π interactions in **CP6**, (c) TOPOS[9] diagram of the offset packed grids.

It is clear from the above crystallographic description that most of these crystals (**CP1** to **CP4** and **CP6**) crystallized in triclinic $P\bar{1}$ space group, whereas **CP5** crystallized in orthorhombic $Pca2_1$ space group. Basically two kinds of architecture were evident after analyzing all the structures viz. **CP1** and **CP3** showed one-dimensional looped chain topology whereas **CP4**, **CP5**, and **CP6** displayed 2D grid architecture; **CP2** showed a one-dimensional wavy chain structure. These structural diversities among the **CPs** arose because of the flexible nature of the ligands **L1** and **L2** that displayed two different coordination modes (angular and linear). In addition to the ligand flexibility, varied coordination modes of oxalate (bridging and chelating) were also responsible for these structural diversities. It is interesting to note that internetwork hydrogen bonding involving urea synthon is not observed in any of these structures.

Catalysis. CPs acting as catalysts in ring-opening alcoholysis of epoxides have been reported by various groups.[2a,10] To the best of our knowledge, none of the reports dealing with alcoholysis of epoxides involves CP as catalyst wherein the ligand backbone is equipped with hydrogen bonding

functionality (NIB−noninnocent backbone, see Introduction). Since epoxide can participate in hydrogen bonding interactions with urea functionality as depicted in Scheme 3, we thought it

Scheme 3
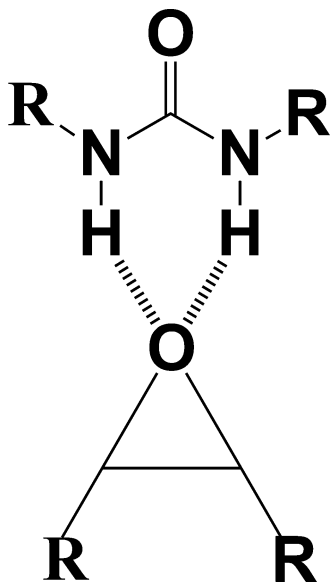
might facilitate the reaction by bringing the substrates (epoxides) in close proximity of the catalytic Cu^{II} metal center in the CPs studied herein. Therefore, we performed methanolysis of various epoxides using the CPs reported herein. Except **CP2**, all the CPs displayed catalytic activity in such reactions (Table 2).

Thus, it is evident from Table 2 that all the CPs acted as excellent catalyst for styrene oxide methanolysis. They also catalyzed the methanolysis of cyclohexene oxide quite efficiently. In the case of *trans*-stilbene oxide, the major product was the methanolysis product, whereas the alpha diketone product (benzil) was the minor one as evident from GC, mass and ^{1}H NMR and ^{13}C NMR (DEPT) analyses. On the other hand, when *cis*-stilbene was used as substrate, the GC-MS showed only one peak for product (benzil). Further analyses (mass and ^{1}H NMR and ^{13}C NMR (DEPT)) revealed that the methanolysis product was also present which could not be detected in the GC trace. It may be mentioned that the alpha diketone product is not commonly observed in methanolysis of stilbene oxides.[11] Both cyclopentene and cyclooctene oxides were found to be unreactive under these catalytic conditions.

As-synthesized CPs did not show any catalytic activity. However, when activated, all of them except **CP2** did display reasonable catalytic properties. Typically, the as-synthesized CP was subjected to heating under a high vacuum at ∼140 °C for about 2 h. In most of the cases, TG data revealed that the lattice included and in some cases, the metal bound solvents except in **CP2**, **CP3** escaped the crystal lattice. The resultant activated catalyst was then placed in a reaction vessel containing the epoxide substrate and MeOH and the mixture was stirred at room temperature. The reaction progress was monitored by GC analyses. Attempt to recycle the catalyst after isolation from the reaction mixture followed by activation was unsuccessful. But if the reaction was performed without isolating the catalyst from the reaction mixture, the reaction (recyclability) was running smoothly, however, with a gradual decrease in the

catalytic efficiency particularly after a third run for **CP4** and **CP5**.

An attempt to correlate the catalytic performances of the CPs based on their crystal structures revealed interesting observations. Since all the CPs displayed nonporous architecture, the catalytic metal center is not expected to be exposed to the upcoming substrate epoxides. Therefore, in order for the CPs to act as catalyst, some kind of changes in the crystalline phases wherein the metal center is somewhat exposed must be happening during the reactions. In fact, a close look at the PXRD patterns of the CPs (simulated, bulk, activated, and reacted) in all the cases displayed considerable differences meaning that the crystal structures of the CPs underwent some change/collapse/degradation; in the cases of **CP1**, **CP3**, and **CP4**, although quite a few peaks do match with that of in the simulated pattern, there still exist considerable differences indicating some kind of change in crystalline phase/degradation in these cases (Figure 7). Thus, these data indicate that a substrate accessible Cu^{II} species might be generating during reaction, which acted as catalyst.

To probe it further, we have carried out EPR experiments on a selected CP, namely, **CP5**. We recorded EPR spectra under three different conditions: (a) **CP5** as synthesized (before using it as catalyst), (b) **CP5** isolated after carrying out methanolysis of styrene oxide, and (c) the mother liquor of the reaction mixture devoid of any solid catalyst. The EPR spectra obtained in conditions (a) and (b) are identical displaying rhombic symmetry having $g_1 = 2.03819$, $g_2 = 2.06912$, and $g_3 = 2.2848$ indicating the existence of Cu^{II} species with its unpaired electron lying in $d_{x^2-y^2}$ orbital with $s = 1/2$ meaning that the Cu^{II} center is square pyramidal as also seen in the single crystal structure of **CP5**. Thus, the coordination of the metal center does not seem to change after reaction. EPR spectrum in condition (c) does not give any characteristic EPR signal meaning that **CP5** is not leaching into the reaction mixture. Therefore, these results indicate that the metal center is getting exposed to the substrate due to some dynamic structural change during the reaction — the exact nature of which could not be established (see Supporting Information).
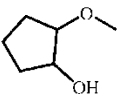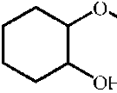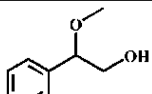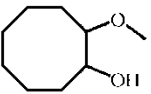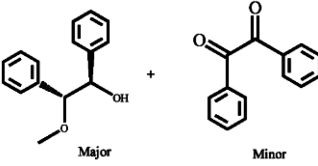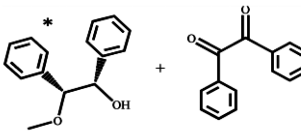
■ CONCLUSIONS

On the basis of crystal engineering rationale, we have synthesized mixed ligand based Cu^{II} coordination polymers **CP1−CP6** derived from bis-pyridyl-bis-urea ligands and various carboxylates. All of them were structurally characterized by single crystal X-ray diffraction. Urea synthon could not be observed in any of these structures. Except **CP2**, all the CPs displayed moderate to excellent epoxide ring-opening methanolysis with various substrates. Styrene oxide turned out to be the best substrate resulting in 100% conversion within 12 h. Since single crystal structures of the these CPs did not display any open channel conducive for ring-opening catalysis and PXRD data under various conditions indicated structural changes/degradation, it is logical to presume that a substrate accessible Cu^{II} species might be generated during reactions, which acted as catalyst.

■ EXPERIMENTAL SECTION

Materials and Methods. All chemicals were commercially available and used without further purification. Ligands **L1** and **L2** were synthesized were previously reported.[7] The elemental analysis was carried out using a Perkin-Elmer 2400 Series-II CHN analyzer. FT-IR spectra were recorded using Perkin-Elmer Spectrum GX, and

**Table 2. Methanolysis of Various Epoxides Catalyzed by CP1, CP3−CP6**

SUBSTRATE	CATALYST				
	CP1	CP3	CP4	CP5	CP6
	PRODUCTS				

Cyclopentene-oxide	Conv. (%) =10 Time = 36 h TON = 1.0 TOF = 0.01 h^{-1}	Conv. (%). = 5 Time = 168 h TON = 0.5 TOF=0.030 h^{-1}	Conv.(%).=32 Time = 36 h TON = 3.2 TOF=0.09 h^{-1}	Conv.(%).=10 Time =168 h TON=1.0 TOF =0.004 h^{-1}	Conv.(%). = 25 Time = 36 h TON = 2.5 TOF = 0.07 h^{-1}

Cyclohexene- oxide	Conv.(%)=92 Time (h)=46 TON=9.2 TOF= 0.2h^{-1}	Conv.(%)=100 Time (h)=45 TON=10 TOF=0.22 h^{-1}	Conv.(%)=100 Time (h)=40 TON=10 TOF=0.25 h^{-1}	Conv.(%)=100 Time (h)=44 TON=10 TOF= 0.22 h^{-1}	Conv.(%)=100 Time (h)=36 TON =10 TOF= 0.277 h^{-1}

Styrene oxide	Conv.(%)=100 Time (h)=12 TON=10 TOF= 0.833h^{-1}	Conv.(%)=100 Time (h)=12 TON=10 TOF=0.833h^{-1}	Conv.(%)=100 Time (h)=6 TON=10 TOF= 0.833 h^{-1}	Conv.(%)=100 Time (h)=3.5 TON=10 TOF= 1.50 h^{-1}	Conv.(%)=100 Time (h)=12 TON = 10 TOF= 0.833 h^{-1}

Cyclooctene- oxide	----------------------------------No Reaction----------------------------------				

Major + Minor

Trans-stilbene oxide	Conv.(%)=100(86,14) Time (h)= 228 TON=10 TOF=0.044 h^{-1}	Conv.(%)=100(72,28) Time (h)=44 TON=10 TOF= 0.23 h^{-1}	Conv.(%)=(23,54) Time (h)=48 TON =7.7 TOF=0.16 h^{-1}	Conv.(%)=100 (32,68) Time (h)=24 TON=10 TOF=0.416 h^{-1}	Conv.(%)=66 (43,23) Time (h)=72 TON =6.6 TOF = 0.1 h^{-1}

* could not be ascertained by GC; ascertained by NMR and Mass

* +

Cis-stilbene oxide	Conv.(%)=31 Time (h)= 108 TON=3.1 TOF =0.028h^{-1}		Conv.(%)=21 Time (h)= 144 TON=2.1 TOF=0.015 h^{-1}	Conv.(%)=53 Time (h)= 72 TON =5.3 TOF=0.074 h^{-1}	Conv.(%)= 91 Time (h)= 228 TON=9.1 TOF=0.039 h^{-1}	Conv.(%)= 27 Time (h)= 120 TON=2.7 TOF=0.023h^{-1}

TGA analyses were performed on a SDT Q Series 600 Universal VA.2E TA Instruments. Powder X-ray patterns were recorded on a Bruker AXS D8 Advance Powder (Cu $K\alpha1$ radiation, λ = 1.5406 Å) diffractometer. GC was recorded on a PERICHROM PR:2100. GCMS was recorded on GCMS-shimazdu-QP 5050A.The mass spectrum was recorded on QTOF Micro YA263. NMR spectra were recorded using a 300 MHz Bruker Avance DPX300 spectrometer EPR spectra was recorded on JES-FA SERIES.

CP1[{Cu(μ-L1)(NO$_3$)(μ-oxalate)$_{0.5}$}(H$_2$O)]$_\infty$ was synthesized by layering an ethanolic solution of L1 (30 mg, 0.1 mmol) over an aqueous solution of diammonium oxalate (4.7 mg, 0.033 mmol) in water and later layering a methanolic solution of Cu(NO$_3$)$_2$ (24 mg, 0.1 mmol). The resultant trilayer solution, thus obtained, was kept undistbed. After 1 week, plate shaped green crystals appeared. Elemental analysis calcd for C15 H20 Cu N7 O9(%): C,35.47; H, 4.37; N, 19.30; found: C 36.25, H 3.70, N 19.20. FT-IR (KBr pellet) 3394m, 3306(m, water ν O−H), 2960w, 2798w, 1699s (urea C═O stretch), 1645s (s, urea C═O stretch), 1589, 1556 (s,urea N−H bending), 1506, 1483, 1429, 1384, 1330, 1924, 1240 (NO$_3$-asymmetric stretch), 1134, 1105, 1068, 937, 906, 804, 694, 653, 615, 495.
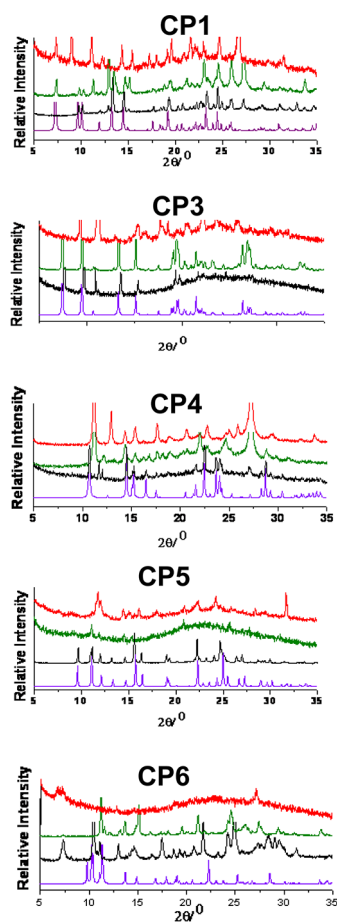
Figure 7. PXRD patterns of **CP1**, **CP3**−**CP6** under various conditions, e.g., simulated (violet), bulk (black), activated (olive), reacted (red).

CP2 [Cu(μ-**L1**)(DMF)$_2$(oxalate)]$_\infty$ was synthesized by layering an DMF solution of **L1** (30 mg, 0.1 mmol) over an aqueous solution of diammonium oxalate (4.7 mg, 0.033 mmol) in water and later layering a ethanolic solution of Cu(NO$_3$)$_2$ (24 mg, 0.1 mmol). The resultant trilayer solution, thus obtained, was kept undisturbed. After 10 days, block shaped green crystals appeared. Elemental analysis calcd C22 H30 Cu N8 O8%: C,44.18; H, 5.06; N, 18.74; found: inconsistent experimental data FT-I.R (KBr pellet): 3389s, 3279s,1707m (urea C═O stretch), 1649s (urea C═O stretch), 1552s (s,urea N−H bending), 1483s, 1427s, 1384w, 1330w, 1300s, 1232s, 1222, 1130, 1111 cm^{-1}.

CP3[{Cu(μ-**L2**)(H$_2$O)(μ-oxalate)$_{0.5}$}NO$_3$]$_\infty$ was synthesized by layering an ethanolic solution of **L2** (31 mg, 0.1 mmol) over an aqueous solution of diammonium oxalate (4.7 mg, 0.033 mmol) in water and later layering a methanolic solution of Cu(NO$_3$)$_2$ (24 mg, 0.1 mmol). The resultant trilayer solution, thus obtained, was kept undisturbed. After 10 days, block-shaped green crystals appeared. Elemental analysis calcd C16 H20 Cu N7 O8 (%): C, 38.21; H, 4.21; N,19.50; found: C, 38.68; H, 3.58;N,19.51; FT-IR (KBr pellet): 3396m, 3333 (m, water ν O−H), 3113w, 1710s (C═O stretch), 1683 (s, N−H bending), 1651s, 1612w, 1587w, 1556s, 1539s, 1494m, 1479m 1423(NO$_3$-asymmetric sretch), 1373w, 1350w, 1319w, 1274w, 1228m, 1215m, 1109, 1064, 1028w, 995w, 809s, 698s, 655m, 640m, 486 m, 457w, 420w cm^{-1}.

CP4[{Cu(μ-**L1**)(H$_2$O)$_2$(μ-succinate)}·H$_2$O]$_\infty$ was synthesized by layering an ethanolic solution of **L1** (30 mg, 0.1 mmol) over an aqueous solution of dipotassium succinate (6.5 mg, 0.033 mmol) in water and later layering a methanolic solution of Cu(NO$_3$)$_2$ (24 mg, 0.1 mmol). The resultant trilayer solution, thus obtained, was kept undisturbed. After 6 days, block shaped blue crystals appeared, calcd. C18 H20 Cu N6 O10 (%): C, 39.17; H, 5.11; N,15.11; found:

experimental data was inconsistent, FT-IR (KBr pellet): 3360 w, 3315w, 3080 (w, aliphatic C−H stretch), 1695m, 1683m (s, urea C═O stretch), 1670 (s, urea C═O stretch), 1585w, 1541s, 1483s, 1425m, 1384s, 1327s, 1300m, 1273s, 1226m, 804 m, 694m cm^{-1}.

CP5[{Cu(μ-**L2**)(H$_2$O)(μ-succinate)}·3H$_2$O]$_\infty$ (**CP5**) was synthesized by layering an ethanolic solution of **L2** (31 mg, 0.1 mmol) over an aqueous solution of dipotassium succinate (6.5 mg, 0.033 mmol) in water and later layering a methanolic solution of Cu(NO$_3$)$_2$ (24 mg, 0.1 mmol). The resultant trilayer solution, thus obtained, was kept undisturbed. After 10 days, neddle shaped blue crystals appeared, Elemental analysis calculated for C19 H30 Cu N6 O10 (%): C 40.32, H 5.32, N 14.85; found: C, 41.17; H, 4.73; N, 15.59; FT-IR (KBr pellet): 3365m 3298m, 3263 (s, aromatic C−H stretch), 3134w, 3080w, 2966w, 2947, 1693s (s, urea C═O stretch), 1683 (s, urea C═O stretch), 1583 (s, urea N−H bend), 1566s, 1487s, 1427s, 1404s, 1327s, 1298s, 1271w, 1234s, 1193 m, 1234s, 1109m, 1060 w, 879w, 806, 696s, 650s, 680w, 609w cm^{-1}.

CP6 [{Cu(μ-**L1**)(μ-2,6-naphthalene-dicarboxylate)-H$_2$O}·2MeOH]$_\infty$ was synthesized by layering an ethanolic solution of **L1** (30 mg, 0.1 mmol) over an aqueous solution of 2,6-dipotassium naphthalene dicarboxylate (7 mg, 0.033 mmol) in water and later layering a methanolic solution of Cu(NO$_3$)$_2$ (24 mg, 0.1 mmol). The resultant trilayer solution, thus obtained, was kept undisturbed. After 1−2 weeks, neddle shaped bluish green crystals appeared. C,H,N experimental data was inconsistent FT-IR (KBr pellet): 3504m, 3389, 3356m, 3082m, 1672s (urea C═O stretch), 1591m (s, urea N−H bend), 1552s, 1514w, 1481s, 1431s, 1384s, 1352s, 1300m, 1265m, 1244m, 1139w, 1116, 1062, 1028, 999w, 918m, 879w, 833w, 821m, 806m, 696s, 655w cm^{-1}.

Catalytic Reaction Conditions. Reaction conditions: All the reactions were carried out at room temperature under vigorous magnetic stirring. Catalyst/substrate (epoxide) ratio was maintained at 1:10. In a typical reaction 6.5×10^{-3} mmol of the catalyst and 6.5×10^{-2} mmol of the epoxide was taken in 5 mL of methanol and stirred at room temperature in a stoppered container.

X-ray Crystallography: X-ray single crystal data were collected using MoKα (λ = 0.7107 Å) radiation on a BRUKER APEX II diffractometer equipped with CCD area detector. Data collection, data reduction, structure solution/refinement were carried out using the software package of APEX II. The structures of **CP1**−**CP6** were solved by direct method, respectively, and refined in a routine manner. In all cases, non-hydrogen atoms were treated anisotropically. Whenever possible, the hydrogen atoms were located on a difference Fourier map and refined. In other cases, the hydrogen atoms were geometrically fixed. CCDC Nos. 885293−885298 contain the supplementary crystallographic data for this paper. These data can be obtained free of charge via www.ccdc.cam.ac.uk/conts/retrieving.html (or from the Cambridge Crystallographic Data Centre, 12 Union Road, Cambridge CB21EZ, UK; fax: (+44) 1223−336−033; or deposit@ccdc.cam.ac.uk).

■ ASSOCIATED CONTENT

ⓢ Supporting Information

Detail experimental conditions, SXRD details and TG curves, PXRD patterns. This material is available free of charge via the Internet at http://pubs.acs.org.

■ AUTHOR INFORMATION

Corresponding Author

*E-mail: parthod123@rediffmail.com, ocpd@iacs.res.in.

Present Addresses

#Department of Inorganic Chemistry, Indian Association for the Cultivation of Science (IACS), 2A and 2B Raja S C Mullick Road, Jadavpur Kolkata −700032, West Bengal, India.
§Institute of Condensed Matter and Nanosciences, Université Catholique de Louvain, Place L. Pasteur 1, 1348 Louvain-la-Neuve, Belgium.

Notes

The authors declare no competing financial interest.

REFERENCES

(1) Janiak, C. *Dalton Trans.* **2003**, 2781.

(2) (a) Jiang, D. M.; Urakawa, A.; Yulikov, M.; Mallat, T.; Jeschke, G.; Baiker, A. *Chem.—Eur. J.* **2009**, *15*, 12255. (b) Hasegawa, S.; Horike, S.; Furukawa, R. S.; Mochizuki, K.; Kinoshita, Y.; Kitagawa, S. *J. Am. Chem. Soc.* **2007**, *129*, 2607. (c) Neogi, S.; Sharma, M.; Bharadwaj, P. K. *J. Mol. Catal. A: Chem.* **2004**, *299*, 1. (d) Ma, L.; Abney, C.; Lin, W. *Chem. Soc. Rev.* **2009**, *38*, 1248.

(3) (a) Kumar, D. K.; Jose, D. A.; Das, A.; Dastidar, P. *Inorg. Chem.* **2005**, *44*, 6933. (b) Uemura, K.; Kitagawa, S.; Kondo, M.; Fukui, K.; Kitaura, R.; Chang, H.-C.; Mizutani, T. *Chem.—Eur. J.* **2002**, *8*, 3587.

(4) Adarsh, N. N.; Dastidar, P. *Chem. Soc. Rev.* **2012**, *41*, 3039.

(5) Kumar, D. K.; Dastidar, P. *Inorg. Chem. Commun.* **2008**, *11*, 636.

(6) (a) Adarsh, N. N.; Dastidar, P. *Cryst. Growth Des.* **2010**, *10*, 4976. (b) Kumar, D. K.; Dastidar, P.; Das, A. *J. Mol. Struct.* **2006**, *796*, 139.

(7) (a) Byrne, P.; Turner, D. R.; Lloyd, G. O.; Clarke, N.; Steed, J. W. *Cryst. Growth Des.* **2008**, *8*, 3335. (b) Adarsh, N. N.; Kumar, D. K.; Dastidar, P. *CrystEngComm* **2008**, *10*, 1565. (c) R. Custelcean, R.; Sellin, V.; Moyer, B. A. *Chem. Commun.* **2007**, 1541.

(8) Spek., A. L. *J. Appl. Crystallogr.* **2003**, *36*, 7.

(9) Blatov, V. A.; Proserpio, D. M. *TOPOS 4.0, A Program Package for Multipurpose Crystallochemical Analysis.*

(10) (a) Hong, S. J.; Ryu, J. Y.; Lee, J. Y.; Kim, C.; Kim, S. J.; Kim, Y. *Dalton Trans.* **2004**, 2697. (b) Dhakshinamoorthy, A.; Alvaro, M.; Garcia, H. *Chem.—Eur. J.* **2010**, *16*, 8530.

(11) Antoniotti, S.; Duñach, E. *J. Mol. Catal. A: Chem.* **2004**, *208*, 135.